Experimental evidence of anapolar moments in the antiferromagnetic insulating phase of V_2O_3 obtained from x-ray resonant Bragg diffraction

J. Fernández-Rodríguez,[1] V. Scagnoli,[1] C. Mazzoli,[1] F. Fabrizi,[1] S. W. Lovesey,[2,3] J. A. Blanco,[4] D. S. Sivia,[5] K. S. Knight,[2] F. de Bergevin,[1] and L. Paolasini[1]

[1]*European Synchrotron Radiation Facility, BP 220, 38043 Grenoble Cedex, France*

[2]*ISIS Facility, Rutherford Appleton Laboratory, Oxfordshire OX11 0QX, United Kingdom*

[3]*Diamond Light Source Ltd., Oxfordshire OX11 0DE, United Kingdom*

[4]*Departamento de Física, Universidad de Oviedo, E-33007 Oviedo, Spain*

[5]*St. John's College, Oxford OX1 3JP, United Kingdom*

(Received 25 November 2009; published 8 February 2010)

We have investigated the antiferromagnetic insulating phase of the Mott-Hubbard insulator vanadium sesquioxide (V_2O_3) by resonant x-ray Bragg diffraction at the vanadium K edge. Combining the information obtained from azimuthal angle scans, linear incoming polarization scans and by fitting collected data to the scattering amplitude derived from the established chemical $I2/a$ and magnetic space groups we provide direct experimental evidence of the ordering motif of vanadium magnetoelectric multipoles in V_2O_3. Experimental data (azimuthal dependence and polarization analysis) collected at space-group forbidden Bragg reflections are successfully accounted within our model in terms of vanadium magnetoelectric multipoles. We demonstrate that resonant x-ray diffraction intensities in all space-group forbidden Bragg reflections of the kind $(hkl)_m$ with odd h are produced by an $E1-E2$ event. The determined multipolar parameters offer a test for *ab initio* calculations in this material, which can lead to a deeper and more quantitative understanding of the physical properties of V_2O_3.

DOI: 10.1103/PhysRevB.81.085107 PACS number(s): 78.70.Ck, 71.30.+h, 75.50.Ee, 78.70.Dm

I. INTRODUCTION

X-ray diffraction is an established experimental technique by which to determine the electronic structure of materials. Resonant enhancement of the scattering amplitude, achieved by tuning the x-ray energy to an atomic resonance gives additional information on charge, orbital, and spin degrees of freedom not accessible to other experimental techniques.[1,2] In the case of ions located in crystal positions that are not a center of inversion symmetry, hybridization will occur between valence orbitals with different parity of that ion as a result of angular anisotropy in the cation's electron distribution from covalency and odd-order contributions in the electrostatic potential. This enables the possibility of observing electronic transitions to the hybridized states via the mixed dipole-quadrupole ($E1-E2$) channel in resonant x-ray scattering,[1,3–6] which is sensitive to the ordering of parity-breaking multipolar moments. For example, the ordering of magnetoelectric anapolar moments might be observed. An orbital anapole moment,[7] constructed from the position operator $\mathbf{r}$ and the orbital angular momentum $\mathbf{L}$ as $\Omega=\mathbf{r}\times\mathbf{L}-\mathbf{L}\times\mathbf{r}$, characterizes a system that does not transform into itself under space inversion. These anapolar moments were initially considered in the context of multipolar expansions in nuclear physics[8] and are related to a distribution of magnetic fields which is quite different from those produced by parity-even multipoles. The magnetoelectric (parity odd and time odd) dipole is equivalent to the nuclear anapole, which has been investigated by atomic parity violation experiments,[9] while the magnetoelectric monopole is equivalent to magnetic charge.[10] The magnetic field distribution of an anapole looks like the magnetic field created by a current flowing in a toroidal winding, and the field is completely confined inside the winding. In the same way as parity-even contributions to resonant scattering can give information on different parity-even multipolar moments,[11–13] dipoles, quadrupoles, hexadecapoles, etc., parity-breaking $E1-E2$ contributions to scattering can be expressed in terms of polar and magnetoelectric tensors that contain the anapole operator.[1] The study of these contributions to resonant x-ray diffraction is of fundamental importance in current developments of the electronic structure of materials with complex electronic properties, such as magnetoelectricity, piezoelectricity, and ferroelectricity that are of potential technological interest.[14] The cross correlation between magnetism and ferroelectricity in materials with coexistence of spontaneous magnetization and polarization, termed multiferroics, has recently become a subject of great scientific impact. Anapolar moments in magnetic ions at noncentrosymmetric sites can play an important role in multiferroic properties. An anapole moment is inherently magnetoelectric.[8] In the classical picture described above of a toroidal solenoid, in the presence of an external magnetic field $\mathbf{H}$, the energy of each spin carrier (electron) depends on its location on the annular orbit, on which the electrons are constrained so that the electron distribution will no longer remain uniform and the external magnetic field will induce an electric polarization $\mathbf{P}$ orthogonal to $\mathbf{H}$.

Vanadium sesquioxide, V_2O_3, considered as a Mott-Hubbard metal-insulator[15] system, has been the object of intense study from both theoretical[16–19] and experimental[20–23] points of view in the last decades. This compound has an interesting phase diagram, with an antiferromagnetic insulating phase (AFI) at low temperatures, and a paramagnetic metallic (PM) one above the Néel temperature ($T_N \approx 150$ K). The metal-insulator transition is accompanied by a first-order structural phase transition in which the room-

temperature corundum structure ($R\bar{3}c$) is modified to monoclinic $I2/a$. In 1978 Castellani, Natoli, and Ranniger[16] proposed a theoretical model to explain the magnetic structure in the AFI phase from the ordering pattern of the occupation of the t_{2g} (degenerate) orbitals. This model was considered valid until 1999, when resonant x-ray diffraction (Paolasini *et al.*[20]), and magnetic dichroism measurements (Park *et al.*[22]) demonstrated that the spin of the Vanadium atoms was $S_V=1$, whereas the model of Castellani predicted $S_V=1/2$.

The magnetic structure is such that the I-centering cell translation is time inverting. Because of the magnetic moments being collinear in the $\mathbf{a}_m-\mathbf{c}_m$ plane, normal magnetic peaks are observed only at reflections $(hkl)_m$ with even h even and odd $(k+l)$. Yet, peaks have been measured at odd h, even $(h+l)$, at the resonant prepeak of the Vanadium K edge. They were initially interpreted as produced by orbital (time even) ordering.[20,21] However, analyses carried out by Lovesey *et al.*[17] and Tanaka[18] demonstrated that the resonant Bragg diffraction intensities are produced by the ordering of magnetic (time odd) V multipoles. There has been controversy on the dominant resonant event producing the measured intensities, having been proposed a parity-even $E2-E2$ event,[17] a parity-odd $E1-E2$ event,[18] or a combination of them.[19,24] In this work, using resonant x-ray diffraction we obtain direct experimental evidence for the vanadium magnetoelectric dipole (anapole) and other magnetoelectric multipoles. A discussion of the selection rules that constrain observable multipoles in reflections $(hkl)_m$ with even h even and odd $(k+l)$ and an orientation to the properties of parity-breaking multipoles are provided in Appendixes A and B.

II. EXPERIMENTAL METHOD

Experiments were carried out on the ID20 beamline[25] at the ESRF. A single crystal of 2.8% Cr-doped $(V_{1-x}Cr_x)_2O_3$ $(x=0.028)$ was mounted on the four-circle diffractometer with vertical scattering geometry. The sample was cooled in a displex cryostat down to 100 K, and a single monoclinic domain was obtained in the beam illuminated area. In addition to standard energy profiles and azimuthal scans of space-group forbidden reflections, measurements based on linear polarization analysis of the scattering beam while varying the direction of the linear polarization of the incoming one, at fixed sample azimuth, were performed. By means of a phase-plate setup[26] we can obtain the Stokes parameters for the secondary beam as a function of both incident and scattered linear polarization angle, without moving the crystal. This method can elucidate the presence of resonances that are very close in energy, playing on their relative phase shifts. To vary the incoming linear polarization, a diamond (111) phase plate of thickness 300 μm was inserted into the incident beam. The phase plate was operated in half-wave plate mode to rotate the incident polarization into an arbitrary plane (see Refs. 27 and 28 and Appendix C) described by Stokes parameters $P_1=\cos(2\eta)$ and $P_2=\sin(2\eta)$, being η the angle between the incident beam electric field and the axis perpendicular to the scattering plane, i.e., $\eta=0$ corresponds to polarization perpendicular to the scattering plane (σ polarization). The

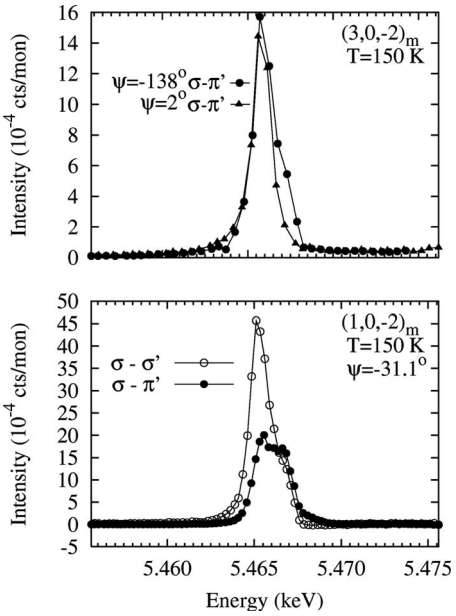

FIG. 1. Measured energy profiles of the $(30\bar{2})_m$ reflection at the azimuthal angles of $\psi=2$ and $\psi=-138$ degrees and $(10\bar{2})_m$ reflection at $\psi=-31.1$ degrees. The origin of the azimuthal angles corresponds to $(010)_m$ reciprocal lattice vector in the plane of scattering.

Poincaré-Stokes parameters are defined by $P_1=(\langle|\boldsymbol{\epsilon}_\sigma|^2\rangle-\langle|\boldsymbol{\epsilon}_\pi|^2\rangle)/P_0$, $P_2=2\,\mathrm{Re}(\langle\boldsymbol{\epsilon}_\sigma^*\boldsymbol{\epsilon}_\pi\rangle)/P_0$, $P_3=2\,\mathrm{Im}(\langle\boldsymbol{\epsilon}_\sigma^*\boldsymbol{\epsilon}_\pi\rangle)/P_0$, with $P_0=\langle|\boldsymbol{\epsilon}_\sigma|^2\rangle+\langle|\boldsymbol{\epsilon}_\pi|^2\rangle$ the total intensity, and where $\boldsymbol{\epsilon}_\sigma$ and $\boldsymbol{\epsilon}_\pi$ are the components of the beam polarization vector perpendicular and parallel to the scattering plane, respectively.

III. RESULTS

We present measurements at space-group forbidden Bragg reflections $(h0l)_m$ with odd h in the low temperature monoclinic phase of V_2O_3. Figure 1 shows the energy profiles for the $(30\bar{2})_m$ and $(10\bar{2})_m$ reflections. They contain a single resonant peak centered around 5.465 keV, as it is expected for reflections $(hkl)_m$ with odd h, in which the resonant peak from 5.47 to 5.49 keV, ascribed to an $E1-E1$ event is forbidden.[17,20,29] Energy profiles in Fig. 1 show the presence of a shoulder at $E=5.4665$ keV for both reflections, which opens the possibility for the existence of two Lorentzians separated by approximately 2 eV contributing to the observed intensity. This energy separation can be related to crystalline electric field energy transfer. The value of 10Dq was estimated as 2.1 eV from RIXS measurements.[23] In order to elucidate the possibility of interference of different Lorentzians we have performed polarization analysis measurements of the dependence of the Stokes parameters of the secondary beam as a function of the angle of primary linear polarization η (Fig. 2). Right panels of Fig. 2 show experimental Stokes parameters collected at different energies in $(10\bar{2})_m$ reflection. The fact that the shapes of the Stokes parameters curves remain unchanged indicates that all contributions to resonant x-ray diffraction have the same tensorial form. Furthermore the presence of multiple Lorentzians at

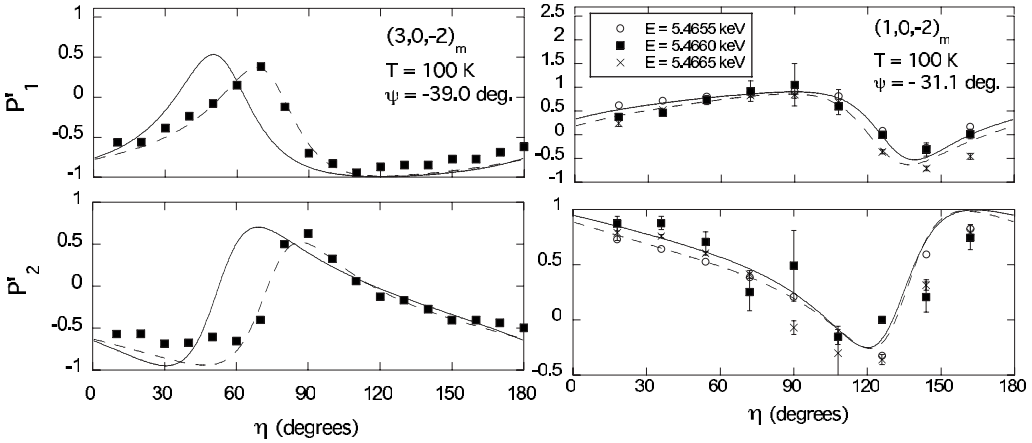

FIG. 2. Linear incident polarization dependence of the Stokes parameters P_1' and P_2' of the secondary beam in the reflections $(30\bar{2})_m(\psi=-39.0$ degrees) collected at $T=100$ K with an incident energy of the x-rays $E=5.4660$ keV and for the reflection $(10\bar{2})_m$ at $\psi=-31.1$ degrees and $T=150$ K and at three different energies $E=5.4655$, 5.4660, and 5.4665 keV. Dashed line corresponds to the fitting of the data to a general Jones matrix produced by a single oscillator including the effect of the phase plate depolarization. Continuous line corresponds to the fitting of polarization data together with azimuthal scans using the parameters presented in Eq. (3). In the origin of the azimuthal angle the $(010)_m$ reciprocal lattice vector is in the plane of scattering.

different energies with different tensorial properties would be revealed by the appearance of a circular component in polarization measurements. Since only the linear polarization is measured, the circular component P_3' (writing P_i and P_i' for incident and diffracted, respectively) can be estimated only as the complement, $P_3'^2=1-P_1'^2-P_2'^2$. But it is then confused with a depolarization, which comes from the imperfect process at the phase plate. This depolarization (see Appendix C) can be accounted by modifying the Stokes parameters of the input polarization. The data actually show some P_3'. In order to check whether this comes from a real circular polarization or from depolarization, they were fitted with a depolarization d parameter and a real Jones matrix (producing no circular component) written in terms of the unit-cell structure factors for the different polarizations $F_{\sigma-\sigma'}$, $F_{\pi-\sigma'}$, $F_{\sigma-\pi'}$, and $F_{\pi-\pi'}$ (formulas for the outgoing Stokes parameters can be seen in Ref. 30). The result is that the occurrence of P_3' is entirely explained from the depolarization, with a value of d, which is consistent with that independently evaluated (see Appendix C). Only one measurement on $(30\bar{2})_m$ shows some discrepancy in d. From the fitting to the $(30\bar{2})_m$ data we obtain the following parameters,

$$d = 0.081 \pm 0.006,$$

$$F_{\pi-\pi'}/F_{\sigma-\sigma'} = 0.8 \pm 0.3,$$

$$F_{\pi-\sigma'}/F_{\sigma-\sigma'} = 0.64 \pm 0.02,$$

$$F_{\sigma-\pi'}/F_{\sigma-\sigma'} = -3.01 \pm 0.05, \quad (1)$$

and from the fitting to the $(10\bar{2})_m$ polarization data we obtain,

$$d = 0.181 \pm 0.007,$$

$$F_{\pi-\pi'}/F_{\sigma-\sigma'} = 0.099 \pm 0.005,$$

$$F_{\pi-\sigma'}/F_{\sigma-\sigma'} = 1.20 \pm 0.01,$$

$$F_{\sigma-\pi'}/F_{\sigma-\sigma'} = 0.770 \pm 0.005. \quad (2)$$

The difference in the values of the depolarization d for $(30\bar{2})_m$ and $(10\bar{2})_m$ reflections does not affect significatively the determined Jones matrix elements. The good agreement obtained in the fittings for both reflections with experimental data for a model, in which we take into account the depolarization introduced by the phase plate, together with the fact that there is no significative dependence of the shape of Stokes parameters curves when the energy of the x-rays is changed in the measurements of $(10\bar{2})_m$ reflection leads us to conclude that there is no evidence of the appearance of circular polarization being the measured intensities in both reflections produced by single oscillators sharing the same tensorial character. All of this supports the validity of fitting the data with a single oscillator model.[19] In this aspect, the model that will be used to describe experimental data differs to the case of K_2CrO_4, where there is a strong evidence of the appearance of circular polarization[26,30] and the intensities were consequently modeled in terms of Lorentzians centered at different energies for the multiple resonant events.

In Fig. 3, we show the azimuthal dependence of $(30\bar{2})_m$ and $(10\bar{2})_m$ reflections measured at $T=100$ K in the AFI phase. In order to eliminate the effect of the absorption in the azimuthal curves, data have been corrected according to the formula

$$I_{\text{corr}} = I_{\text{obs}}(1 + \sin\alpha_0/\sin\alpha_1),$$

where α_0 and α_1 are the incident and reflected angles of the beam with the sample. The measured azimuthal dependence of $(30\bar{2})_m$ shows a satisfactory agreement with previously published data,[19] as shown the two left panels of Fig. 3.

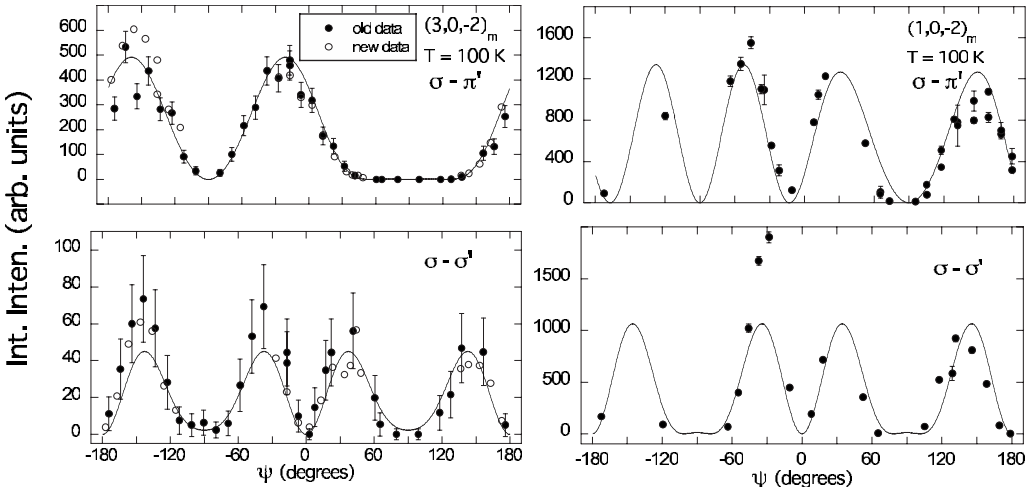

FIG. 3. Azimuthal angle scans measured on the reflections $(30\bar{2})_m$ and $(10\bar{2})_m$ at $T=100$ K with energy $E=5.4665$ keV. In the case of $(30\bar{2})_m$ we show the agreement of new data with previously published data (Ref. 19). The continuous line correspond to the fitting to the expressions for the $F(E1-E2)$ scattering length presented in Ref. 19 with the tensorial parameters shown in Eq. (3). At the origin of the azimuthal angle $(010)_m$ reciprocal lattice vector is in the plane of scattering. Both polarization channels $\sigma-\sigma'$ and $\sigma-\pi'$ are shown.

IV. DISCUSSION

The azimuthal dependence and polarization data collected for $(10\bar{2})_m$ reflection present a good agreement with the expression for the parity-breaking event resonant x-ray scattering $F(E1-E2)$ in terms of magnetoelectric tensors (see Appendix A) presented in Ref. 19, being possible to fit together polarization scans curves and azimuthal data. The azimuthal and polarization data for the $(30\bar{2})_m$ reflection can also be fitted to the $E1-E2$ structure factor expressions together with $(10\bar{2})_m$ data in terms of the same set of parameters, which permits us to conclude that intensities in both $(30\bar{2})_m$ and $(10\bar{2})_m$ are produced by an $E1-E2$ event. The result of the fitting is shown in Figs. 2 and 3. Some discrepancy still exists between experimental data and the fitted intensities, due to many causes: the possibility of variation of the diffraction volume when the sample is rotated, the beam hitting partly other domains of the sample, difficulty in estimating precisely the normal to the surface of the crystal for calculating the absorption correction, etc. The determined parameters from fitting $|F(E1-E2)|^2$ to the experimental data are,

$$\begin{aligned}
\mathrm{Im}\langle G_1^1\rangle/\mathrm{Im}\langle G_3^3\rangle &= 0.263 \pm 0.013,\\
\langle G_0^1\rangle/\mathrm{Im}\langle G_3^3\rangle &= 3.48 \pm 0.06,\\
\mathrm{Im}\langle G_2^2\rangle/\mathrm{Im}\langle G_3^3\rangle &= -8.38 \pm 0.02,\\
\mathrm{Re}\langle G_1^2\rangle/\mathrm{Im}\langle G_3^3\rangle &= 3.908 \pm 0.013,\\
\mathrm{Re}\langle G_2^3\rangle/\mathrm{Im}\langle G_3^3\rangle &= -0.205 \pm 0.007,\\
\mathrm{Im}\langle G_1^3\rangle/\mathrm{Im}\langle G_3^3\rangle &= -3.410 \pm 0.015,\\
\langle G_0^3\rangle/\mathrm{Im}\langle G_3^3\rangle &= -4.33 \pm 0.03. \qquad (3)
\end{aligned}$$

Values for $\mathrm{Im}\langle G_1^1\rangle$ and $\langle G_0^1\rangle$ are direct estimates of the orbital anapolar moment $\langle\Omega\rangle$, $\mathrm{Im}\langle G_3^3\rangle$, $\mathrm{Re}\langle G_2^3\rangle$, $\mathrm{Im}\langle G_1^3\rangle$ and $\langle G_0^3\rangle$ are estimates of the moment $\langle(\mathbf{L}\otimes(\mathbf{L}\otimes\mathbf{\Omega})^2)^3\rangle$, where $\mathbf{L}$ is the operator for orbital angular momentum, and $\mathrm{Im}\langle G_2^2\rangle$ and $\mathrm{Re}\langle G_1^2\rangle$ are estimates of the moment $\langle(\mathbf{L}\otimes\mathbf{n})^2\rangle$, where $\mathbf{n}=\mathbf{r}/r$ is the polar unit vector collinear with the electric dipole moment, and which is even with respect to time-reversal symmetry. Operators $\mathbf{\Omega}$ and $[\mathbf{L}\otimes(\mathbf{L}\otimes\mathbf{\Omega})^2]^3$ are true spherical tensors (they are tensors with odd rank that are space-inversion odd) while $(\mathbf{L}\otimes\mathbf{n})^2$ is a pseudospherical tensor (a tensor with even rank that is space-inversion odd). Additional information about parity-odd tensors may be found in Refs. 1, 7, 8, 10, and 31. The presence of a parity-even contribution $F(E2-E2)$ to resonant x-ray scattering in this kind of reflections has been suggested[17,19,24] and within measured reflections its strongest contribution would appear in the reflection $(30\bar{2})_m$ as $F(E2-E2)$ is weighted by a global multiplicative factor $\sin\nu$, with $\nu=hx+ky+lz$, being x, y, and z crystallographic parameters and the h, k, and l the Miller indices of the reflection.[19] However, our fitting describes data in $(30\bar{2})_m$ with great precision, which makes us conclude that parity-even $E2-E2$ contribution is absent to a good degree of approximation. It has not been possible to fit $(30\bar{2})_m$ and $(10\bar{2})_m$ data together with azimuthal data for reflections $(111)_m$ and $(3\bar{1}1)_m$ given in Refs. 20 and 21. A possible justification are additional contributions present in reflections $(hkl)_m$ with $k\neq 0$, which were neglected in previous analysis due to the approximation $\epsilon=4\pi yk\approx 0$, being $y=0.0008$ a crystallographic parameter (see Refs. 17 and 19). However, although those contributions be proportional to $\sin\epsilon$, among them it is the main component of the vanadium orbital angular momentum $\langle L_0^1\rangle_{(\xi\eta\zeta)}$ with the local axis ζ along the angular momentum direction, which would be of bigger order of magnitude than the tensors observed in $(h0l)_m$ reflections.

Multipoles are defined with respect to quantization axes for our chosen reference site, with the x axis parallel to $\mathbf{b}_m$, and y and z contained in the $\mathbf{a}_m-\mathbf{c}_m$ monoclinic plane with z

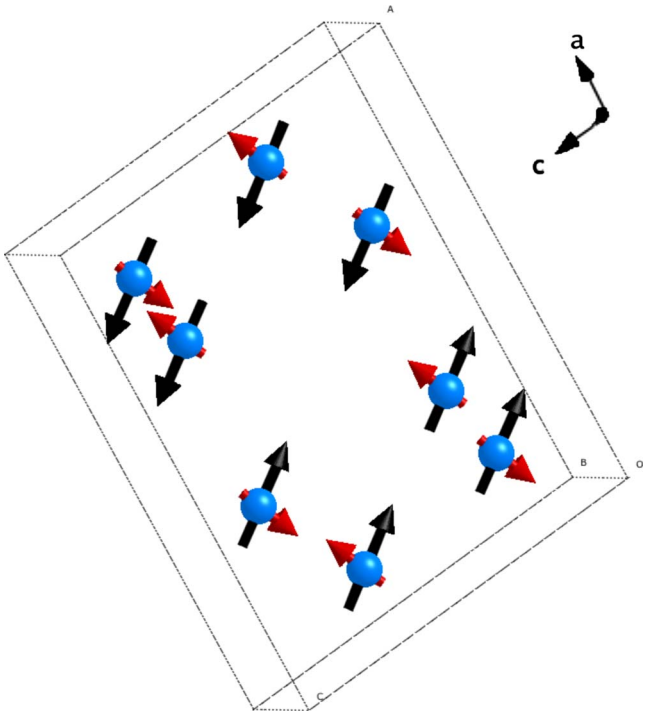

FIG. 4. (Color online) Positions of the Vanadium ions in the monoclinic unit cell adopted by V_2O_3 below the Neel temperature, together with the configuration of the magnetic moments (Ref. 32) (small red arrows) and the determined projection of their anapolar moments (large black arrows) in the $\mathbf{a}_m-\mathbf{c}_m$ plane. The basis vector $\mathbf{b}_m$ is normal to the plane of the diagram.

parallel to $\mathbf{a}_m-\mathbf{c}_m$ and y parallel to $\mathbf{a}_m+2\mathbf{c}_m$. From the fitted parameters, we can determine the direction of the projection in the $\mathbf{a}_m-\mathbf{c}_m$ monoclinic plane of the anapolar moments of the Vanadium ions, which from the quotient between $\mathrm{Im}\langle G_1^1\rangle$ and $\langle G_0^1\rangle$ is estimated as forming 4 degrees with the $(10\bar{1})_m$ reciprocal lattice vector. In Fig. 4, we show the projection in the $\mathbf{a}_m-\mathbf{c}_m$ plane of the anapolar moments of the eight vanadium ions in the monoclinic unit cell, together with the arrangement of magnetic moments[32] established below T_N.

The observation of the magnetoelectric tensors $\langle \mathbf{G}^K\rangle$ implies a substantial parity-mixing between d and p vanadium orbitals, which results from angular anisotropy in the cation's electron distribution from covalency and odd-order contributions in the electrostatic potential. As the local environment of the vanadium ions is not spherically symmetric, angular momentum is not a good quantum number and the ground state is a mixture of various angular momenta. These operators describe the mixing between parity-even and parity-odd orbitals in the ground state. In Appendix B, we have calculated the mean values of these operators for a simple model.

V. CONCLUSIONS

We have shown that it is possible to detect by means of resonant x-ray scattering (RXS) the magnetic anapolar moments and higher order time-reversal and parity-odd multipoles. Resonant x-ray diffraction can give unique access to the local orbital anapole at the resonant site, and can be used to unravel parity-odd properties in solids. The determined values of the magnetoelectric tensors are highly sensitive probes of the cation's electronic state, which cannot be obtained by other experimental methods. These effects are unique probes of the electronic structure. Our results demonstrate that resonant x-ray diffraction at the V K edge for space-group forbidden Bragg reflections of the kind $(h0l)_m$ with odd h is produced by a parity-breaking $E1-E2$ event, being the contribution from parity-even transitions absent to a very good degree of approximation. Polarization analysis measurements at the $(30\bar{2})_m$ and $(10\bar{2})_m$ reflections probe the fact that the intensities measured are coming with a good degree of approximation from single Lorentzians. Experimental data (azimuthal variation and polarization analysis) collected at different space-group forbidden Bragg reflections are successfully accounted within our model in terms of expectation values for the V magnetoelectric multipoles $\langle \mathbf{G}^K\rangle$; these are atomic multipolar moments that are time odd and parity odd for all values of the rank K. The derived parameters include direct estimates of expectation values of the vanadium anapolar moment and other magneto electric moments.[19] These results solve the controversy on the origin of the resonant x-ray diffraction intensities in V_2O_3.[17–19,24] The derived parameters offer a test for *ab initio* calculations of the electronic structure of vanadium sesquioxide that can lead to a deeper and more quantitative understanding of its electronic properties.

ACKNOWLEDGMENTS

We acknowledge useful discussions with Carsten Deflets. Financial support has been received from Spanish MECD under Grant No. MAT2008-06542-C04-03. One of us, J.F.R. is grateful to Gobierno del Principado de Asturias for the financial support from Plan de Ciencia, Tecnología e Innovación (PCTI) de Asturias 2006-2009.

APPENDIX A: UNIT CELL STRUCTURE FACTORS FOR PARITY-EVEN AND PARITY-ODD MULTIPOLES IN $V2_2O_3$

Intensity observed at space-group forbidden reflections is taken to be directly proportional to $|F|^2$ where F is the calculated unit-cell structure factor. The generic form of the unit-cell structure factor F for a given resonant event is,[1]

$$F=\sum_K \mathbf{X}^K\cdot\mathbf{\Psi}^K(h,k,l). \tag{A1}$$

Here, K is the rank of a spherical tensor. Values of K that appear in the sum are determined by the order, or rank, of the resonant processes; from the triangle rule it follows that, $K=1$, 2, and 3 for $E1-E2$ and $K=0$, 1, 2, 3, and 4 for $E2-E2$. One sees in Eq. (A1) that F is the sum of scalar products $\mathbf{X}^K\cdot\mathbf{\Psi}^K(h,k,l)$, in which $\mathbf{X}^K$ describes properties of the primary and secondary x-rays and $\mathbf{\Psi}^K(h,k,l)$ is a structure factor which represents the electron degrees of freedom that contribute to Bragg diffraction at the reflection $(h,k,l)_m$.

Representation of the electron degrees of freedom is achieved with an expectation value, denoted here by angular

brackets, $\langle\ \rangle$, of appropriate atomic spherical-tensor operators, with rank K, that are often called multipoles. We denote parity-even tensors for $E2-E2$ events by $\mathbf{T}^K$, and the corresponding structure factor is,

$$\mathbf{\Psi}^{K,T}(h,k,l) = \sum_{\mathbf{d}} \langle \mathbf{T}^K \rangle_{\mathbf{d}} \exp\, i\mathbf{d}\cdot\tau_m. \tag{A2}$$

In this expression, $\mathbf{d}$ is the position in the unit cell of a resonant vanadium ion and $\tau_m = \tau_m(hkl)$ is the Bragg wave vector. Elements of symmetry in the space and magnetic groups relate multipoles, $\langle \mathbf{T}^K \rangle_{\mathbf{d}}$, at different sites in the unit cell. Full details of the evaluation of Eq. (A2) and $F(E2-E2)$ can be found in Refs. 17 and 19. For parity-even tensors, the structure factor is:

$$\Psi_Q^{K,T} = 2[1+(-1)^{h+k+l+K}]\{\cos\,\nu\langle T_Q^K\rangle + (-1)^h \cos(\nu-\epsilon)\langle T_{-Q}^K\rangle\} \tag{A3}$$

where ν and ϵ are $\nu = 2\pi(x,y,z)_m \tau_m(hkl) = 2\pi(xh+ky+zl)$ and $\epsilon = 4\pi yk$. The factor $[1+(-1)^{h+k+l+K}]$ establishes a selection rule on the rank K of observable tensors in space group forbidden reflections (those with $h+k+l=$odd).

Turning to $E1-E2$ resonant events, two tensor operators represent electron degrees of freedom in the parity-odd channel of scattering, namely, time even and time-odd tensors that we denote by $\mathbf{U}^K$ (polar) and $\mathbf{G}^K$ (magnetoelectric), respectively. The projection Q of a tensor satisfies $-K \le Q \le K$. All values of Q are allowed in the AFI phase because V sites in the monoclinic cell contain no axes of rotation symmetry. Starting from Eq. (A2) and replacing $\mathbf{T}^K$ by either $\mathbf{U}^K$ or $\mathbf{G}^K$, we obtain for $\Psi_Q^{K,U}$ and $\Psi_Q^{K,G}$,

$$\Psi_Q^{K,U} = 2i[1+(-1)^{h+k+l}]\{\sin\,\nu\langle U_Q^K\rangle + (-1)^{K+h}\sin(\nu-\epsilon) \times\langle U_{-Q}^K\rangle\},$$

$$\Psi_Q^{K,G} = 2i[-1+(-1)^{h+k+l}]\{\sin\,\nu\langle G_Q^K\rangle + (-1)^{K+h}\sin(\nu-\epsilon) \times\langle G_{-Q}^K\rangle\}. \tag{A4}$$

In space group forbidden reflections with $h+k+l=$odd time-even tensors U_Q^K are not observable because of the prefactor $[1+(-1)^{h+k+l}]$. U_Q^K are observable in Templeton reflections $(h,0,-h)_m$ with $h=$odd. At space-group forbidden reflections of interest here, the polar structure factor is zero on account of $[1+(-1)^{h+k+l}]=0$ with odd $h+k+l$. Thus, in this set of space-group forbidden reflections, scattering at space-group forbidden reflections is due to time-odd multipoles. $F(E1-E2)$ is derived from $\Psi_Q^{K,G}$. Corresponding unit-cell structure factors in the rotated $(\pi'\sigma)$ and the unrotated $(\sigma'\sigma)$ polarization channels can be found in ref. 19.

APPENDIX B: PARITY-BREAKING MULTIPOLES

Contributions to resonant x-ray diffraction enhanced by the $E1-E2$ event are explored with a model wave function for the equilibrium, ground state of a resonant ion. The wave function chosen is an admixture of p-like and d-like single-particle, atomic states. Mixing parameters may originate from several sources including odd-order contributions to the crystal electric field and covalency. There are two d states, with angular symmetry yz plus z^2. For a p-state we choose $|l',0\rangle$ with angular momentum $l'=1$, which has z-like angular symmetry and no orbital angular momentum because the projection $m'=0$. Mixture of the states $|l,m\rangle$ and $|l',0\rangle$ with $l=2$ and $l'=1$ in the wave function allow parity-odd multipoles to be different from zero. Electron spin is saturated with a wave function $|s=1/2,\ m_s=1/2\rangle$. The complete wave function for the resonant ion is a product state,

$$|\Psi\rangle = \aleph^{1/2}\{|l,0\rangle + ib(|l,+1\rangle + |l,-1\rangle)/\sqrt{2} + f|l',0\rangle\}|s = 1/2,\ m_s = 1/2\rangle, \tag{B1}$$

with the normalization $\aleph$ determined by $\aleph(1+b^2+|f|^2)=1$. In Eq. (B1), the parameter f is allowed to be a complex number, $f=f'+if''$, and it measures mixing of two states with opposite parity.

To learn more about the model wave function we consider expectation values of different operators. The parameter b in Eq. (B1) is chosen to be purely real and consequently expectation values of the orbital angular momentum are zero, i.e., $\langle L_\beta\rangle = 0$ for $\beta = x,y,z$. Thus components of the magnetic moment, $\mu = (\mathbf{L}+2\mathbf{S})$, are $\langle\mu_\beta\rangle = 0$ for $\beta = x,y$, and $\langle\mu_z\rangle = \langle\mu_0\rangle = 1$.

Next, consider expectation values of parity-odd operators allowed by the mixing parameter f. Components of the anapole formed with μ and $\mathbf{r}$ possessed by the state [Eq. (B1)] are,

$$\langle\Omega_x\rangle = \frac{-4\aleph b f'}{\sqrt{5}},$$

$$\langle\Omega_y\rangle = \frac{-8\aleph b f''}{\sqrt{5}},$$

$$\langle\Omega_z\rangle = \langle\Omega_0\rangle = \frac{-16\aleph f''}{\sqrt{15}}. \tag{B2}$$

Finally, consider diagonal components $(Q=0)$ of magnetoelectric multipoles that arise in $E1-E2$ structure factors, for rank 1 and 3. We give results for absorption at a K edge. One finds,

$$\langle G_0^1\rangle = \frac{-\aleph f''}{3\sqrt{5}},$$

$$\langle G_0^3\rangle = (\aleph/3) f'' \sqrt{\frac{7}{15}}, \tag{B3}$$

Like $\langle\Omega_0\rangle$ in Eq. (B2) these multipoles are proportional to the imaginary part of the mixing parameter, f''. Notably, $\langle G_0^1\rangle$ and $\langle G_0^3\rangle$ have similar magnitude.

APPENDIX C: ROTATION OF THE LINEAR POLARIZATION BY A PHASE PLATE, AND DEPOLARIZATION EFFECT

An x-ray phase plate is a crystal near a position of Bragg scattering for a reciprocal lattice point $\mathbf{K}$. Given a reference

frame $(\mathbf{x},\mathbf{y})$ in a plane normal to the beam, the plane of scattering makes an angle χ with $\mathbf{x}$. In that plane, $\mathbf{K}$ is at an angular offset $\Delta\theta$ from the exact Bragg position. Because of this near Bragg condition, the transmitted radiation undergoes an outphase $\phi \propto 1/\Delta\theta$ of its field normal to the plane of scattering with respect to the in plane. With Stokes parameters defined in the $(\mathbf{x},\mathbf{y})$ frame, and the incident beam totally polarized along $\mathbf{x}(P_1=1)$, these parameters are, after the plate,

$$P_1 = \cos^2\frac{\phi}{2} + \sin^2\frac{\phi}{2}\cos 4\chi,$$

$$P_2 = \sin^2\frac{\phi}{2}\sin 4\chi,$$

$$P_3 = \sin\phi \sin 2\chi.$$

By controlling χ and $\Delta\theta$, and then ϕ, any polarization state can be obtained. For a rotated linear polarization, ϕ is fixed to π, the half-wave shift. Then the transmitted linear polarization is at an angle $\eta=2\chi$ with the axis X, since $P_2/P_1 = \tan 4\chi$. In reality the transmitted radiation is not fully polarized because of angular aperture and spectral width of the incident beam, which results into a spread in different rays of out phase $\phi+\delta\phi$. We define as a depolarization parameter $d=\langle(\delta\phi)^2\rangle/2$. By an expansion of the above formulas we have, to the lowest order in $\delta\phi$ (given $\langle\delta\phi\rangle=0$),

$$P_1 = \cos 2\eta + d \sin^2 \eta,$$

$$P_2 = \sin 2\eta - \frac{d}{2}\sin 2\eta.$$

The total linear polarization P_l, defined by $P_l^2=P_1^2+P_2^2$ is degraded as $P_l=1-d\sin^2\eta$. Also it is observed that, P_2/P_1 being different from $\tan 2\eta$, the angle η of that polarization is shifted by $-(d/4)\sin 2\eta$. Indeed, an expansion to first order in d yields,

$$\frac{P_2}{P_1} = \tan 2\left(\eta - \frac{d\sin 2\eta}{4}\right).$$

The depolarization parameter d can be measured in the beam, provided that the sample is removed. It can also be estimated less accurately in line, from the indications of two intensity monitors, before and after the phase plate. In the present experiments, these estimates range between 0.12 and 0.18.

[1] S. W. Lovesey, E. Balcar, K. S. Knight, and J. Fernández- Rodríguez, Phys. Rep. **411**, 233 (2005).
[2] D. H. Templeton and L. K. Templeton, Phys. Rev. B **49**, 14850 (1994).
[3] S. Di Matteo, Y. Joly, A. Bombardi, L. Paolasini, F. de Bergevin, and C. R. Natoli, Phys. Rev. Lett. **91**, 257402 (2003).
[4] I. Marri and P. Carra, Phys. Rev. B **69**, 113101 (2004).
[5] J. Igarashi and T. Nagao, J. Phys. Soc. Jpn. **77**, 084706 (2008).
[6] J. Kokubun, A. Watanabe, M. Uehara, Y. Ninomiya, H. Sawai, N. Momozawa, K. Ishida, and V. E. Dmitrienko, Phys. Rev. B **78**, 115112 (2008).
[7] P. Carra and R. Benoist, Phys. Rev. B **62**, R7703 (2000).
[8] V. M. Dubovik and V. V. Tugushev, Phys. Rep. **187**, 145 (1990).
[9] K. Tsigutkin, D. Dounas-Frazer, A. Family, J. Stalnaker, V. Yashchuk, and D. Budker, Phys. Rev. Lett. **103**, 071601 (2009).
[10] S. W. Lovesey and V. Scagnoli, J. Phys.: Condens. Matter **21**, 474214 (2009).
[11] Y. Tanaka, T. Inami, S. W. Lovesey, K. S. Knight, F. Yakhou, D. Mannix, J. Kokubun, M. Kanazawa, K. Ishida, S. Nanao, T. Nakamura, H. Yamauchi, H. Onodera, K. Ohoyama, and Y. Yamaguchi, Phys. Rev. B **69**, 024417 (2004).
[12] J. Fernández-Rodríguez, J. A. Blanco, P. J. Brown, K. Katsumata, A. Kikkawa, F. Iga, and S. Michimura, Phys. Rev. B **72**, 052407 (2005).
[13] J. Fernandez-Rodriguez, A. Mirone, and U. Staub, J. Phys.: Condens. Matter **22**, 016001 (2010).
[14] T. Lottermoser, T. Lonkai, U. Amann, D. Hohlwein, J. Ihringer, and M. Fiebig, Nature (London) **430**, 541 (2004).
[15] N. F. Mott, *Metal-Insulator Transitions* (Taylor and Francis, London, 1974).
[16] C. Castellani, C. R. Natoli, and J. Ranninger, Phys. Rev. B **18**, 4945 (1978).
[17] S. W. Lovesey, K. S. Knight, and D. S. Sivia, Phys. Rev. B **65**, 224402 (2002).
[18] A. Tanaka, J. Phys. Soc. Jpn. **71**, 1091 (2002).
[19] S. W. Lovesey, J. Fernandez-Rodriguez, J. A. Blanco, D. S. Sivia, K. S. Knight, and L. Paolasini, Phys. Rev. B **75**, 014409 (2007).
[20] L. Paolasini *et al.*, Phys. Rev. Lett. **82**, 4719 (1999).
[21] L. Paolasini, S. D. Matteo, C. Vettier, F. de Bergevin, A. Sollier, W. Neubeck, F. Yakhou, P. Metcalf, and J. Honig, J. Electron Spectrosc. Relat. Phenom. **120**, 1 (2001).
[22] J.-H. Park, L. H. Tjeng, A. Tanaka, J. W. Allen, C. T. Chen, P. Metcalf, J. M. Honig, F. M. F. de Groot, and G. A. Sawatzky, Phys. Rev. B **61**, 11506 (2000).
[23] C. F. Hague, J.-M. Mariot, V. Ilakovac, R. Delaunay, M. Marsi, M. Sacchi, J.-P. Rueff, and W. Felsch, Phys. Rev. B **77**, 045132 (2008).
[24] Y. Joly, S. D. Matteo, and C. R. Natoli, Phys. Rev. B **69**, 224401 (2004).
[25] L. Paolasini *et al.*, J. Synchrotron Radiat. **14**, 301 (2007).
[26] C. Mazzoli, S. B. Wilkins, S. D. Matteo, B. Detlefs, C. Detlefs, V. Scagnoli, L. Paolasini, and P. Ghigna, Phys. Rev. B **76**, 195118 (2007).
[27] C. Giles, C. Vettier, F. de Bergevin, C. Malgrange, G. Grubel, and F. Grossi, Rev. Sci. Instrum. **66**, 1518 (1995).
[28] V. Scagnoli, C. Mazzoli, P. Bernard, A. Fondacaro, L. Paolasini, C. Detlefs, F. Fabrizi, and F. de Bergevin, J. Synchrotron Radiat. **16**, 778 (2009).
[29] S. W. Lovesey and K. S. Knight, J. Phys.: Condens. Matter **12**, L367 (2000).
[30] J. Fernández-Rodríguez, S. W. Lovesey, and J. A. Blanco, Phys. Rev. B **77**, 094441 (2008).
[31] P. Carra, A. Jerez, and I. Marri, Phys. Rev. B **67**, 045111 (2003).
[32] R. M. Moon, Phys. Rev. Lett. **25**, 527 (1970).